Research Article | Vol. 10, No. 8 | 1 Aug 2019 | BIOMEDICAL OPTICS EXPRESS 4290
Biomedical Optics EXPRESS

Identification and investigation of the vibrational properties of crystalline and co-amorphous drugs with Raman and terahertz spectroscopy

Wei Liu,[1,2] Yu Liu,[2] Jiaoqi Huang,[2] Zhongquan Lin,[2] Xuancheng Pan,[3] Xiaojun Zeng,[2] Marc Lamy de la Chapelle,[4] Yang Zhang,[2,5] Weiling Fu[2,*]

[1]*Faculty of Materials and Energy, Southwest University, Chongqing 400715, China*
[2]*Department of Laboratory Medicine, Southwest Hospital, the Army Military Medical University, Chongqing 400038, China*
[3]*Wuhan Life Origin Biotech Joint Stock, Wuhan 430206, China*
[4]*Institut des Molécules et Matériaux du Mans (IMMM-UMR CNRS 6283), Université du Mans, Avenue Olivier Messiaen, 72085 Le Mans, France*
[5]*millen001@163.com*
**fwl@tmmu.edu.cn*

Abstract: Co-amorphous drugs have shown significant potential in improving the stability and bioavailability compared with single neat amorphous drugs. Here, we explored the molecular interactions of cimetidine, naproxen, indomethacin and their binary co-amorphous mixtures via Raman and terahertz (THz) spectroscopy. We used quench-cooled method to prepare the neat amorphous drugs and their binary co-amorphous mixtures and tested their thermodynamic properties through differential scanning calorimetry (DSC). Then, we found that the stability of co-amorphous drugs was stronger than their neat amorphous components. Furthermore, Raman spectroscopy was used to characterize the vibrational modes between different co-amorphous drugs. Generally, we found that the stability of co-amorphous drugs was better than their neat amorphous components for these samples we tested. Meanwhile, we complemented the detection of THz spectroscopy and found that crystalline and amorphous drugs could be better distinguished.

1. Introduction

Nowadays, it is estimated that more than 90% of drugs under development are expected to be poorly water soluble [1,2]. Therefore, amorphous drugs have been generated considerable interest in the pharmaceutical field to overcome the shortcomings of poorly water-soluble drugs. Due to its higher internal energy, amorphous materials have higher solubility and dissolution rate than its crystalline counterparts. Nevertheless, the stability of the amorphous form is relatively poor [3–6]. To improve their stability, co-amorphous drugs have emerged. Co-amorphous drugs are the combination of two or more components with low molecular weight to form a homogeneous amorphous system [4–7]. And the co-amorphous drugs exhibit improved physical stability and dissolution rate compared with neat amorphous drugs. Pharmacologically related drugs can be stabilized by each other through combining them into co-amorphous forms. Therefore, both drugs act as the active ingredients and the stabilizing excipients at the same time.

Most of the studies are based on a basic understanding of co-amorphous formulations, such as their stable situations and behaviors during dissolution situation [8–15]. However, little is known about the vibrational properties of these systems in molecular level, including the molecular interactions among the components of the co-amorphous mixtures. And ideal

#364731 https://doi.org/10.1364/BOE.10.004290
Journal © 2019 Received 10 Apr 2019; revised 16 Jun 2019; accepted 16 Jun 2019; published 31 Jul 2019

Biomedical Optics EXPRESS

co-amorphous drugs cannot be prepared with any small molecule compounds. In some studies, amino acids were used as excipients and that certain amino acids can be successfully stabilized in their amorphous form with one drug were found, but not necessary for other drugs [16]. To find a good co-former, it is crucial to explore the molecular interactions in the co-amorphous drug systems.

The amorphous form materials have raised an enormous challenge to structural analysis. Only little information can be obtained through traditional methods, such as X-ray powder diffraction (XRPD) detection. However, some vibrational spectroscopy techniques, such as Raman and THz spectroscopy, are capable to provide more valuable vibrational properties for solid state characterization, such as intermolecular interactions. Raman spectroscopy is a technique based on the Raman scattering effect and is used to analyze the vibrations of various materials [17]. At the same time, THz absorption spectroscopy is a great method to explore the structure and the interactions of some compounds in the low wavenumber range (lower than 100 cm^{-1}) [18], and it is ultra-sensitive to weak intermolecular interactions.

In this study, we studied 3 kinds of co-amorphous drug combinations among cimetidine, naproxen and indomethacin. Naproxen and indomethacin are non-steroidal anti-inflammatory drugs (NSAIDs) and in this regard are pharmacologically complementary in their use in pain relief. However, it is known that NSAIDs sometimes have side effects such as gastrointestinal disturbances and headache [19]. The H_2-receptor antagonist, cimetidine, has widely used in the treatment of patients with gastrointestinal dysfunction and used to counteract the gastric erosion occurs as side effects resulting from NSAID therapy [20]. As a result, cimetidine may be administered for treating NSAID-induced gastro-intestinal disorders such as those caused by naproxen and indomethacin. We also investigated the thermodynamic properties of these interrelated binary co-amorphous drugs. The interactions between the molecules of the amorphous drugs were explored through Raman spectroscopy. And the results indicated that the molecular interactions between different amorphous forms were the crucial factor affecting the stability of co-amorphous drugs. Furthermore, we detected it with THz spectroscopy and found crystalline and amorphous drugs could be distinguished in higher resolution. In conclusion, we compared a variety of related co-amorphous drug systems in solid state properties and stability analysis under the same preparation and storage conditions. We also proposed some explanations of the molecular interaction mechanisms in co-amorphous systems through multispectral detection. We believe our work will pave the way for a better choice of drug components to improve the stability of their amorphous form.

2. Experimental section

2.1 Materials

Cimetidine (CIM, polymorph A; M = 252.3 g/mol), naproxen (NAP, M = 230.2 g/mol), indomethacin (IND, polymorph γ; M = 357.8 g/mol) were purchased from Sigma Aldrich. Their chemical structures are shown in Fig. 1. All of the drugs are at analytically pure grade.

Biomedical Optics EXPRESS

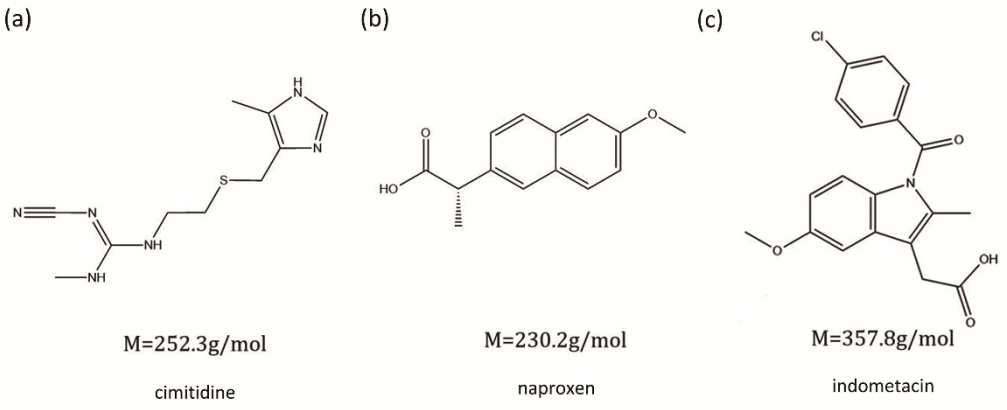

Fig. 1. Chemical structures of (a) CIM, (b) NAP and (c) IND.

2.2 The preparation of neat amorphous drugs and co-amorphous drugs

Neat amorphous drugs of CIM, NAP and IND and their binary co-amorphous mixtures (CIM-NAP, CIM-IND, NAP-IND) were prepared with quench-cooled method [21]. Neat sample powder (0.5 g) was spread in an aluminum pan and melted at approximately 170 °C with a heating plate. Then the pan with the melted drugs was immersed into liquid nitrogen for 3 minutes. The cooled drugs need to be scraped off and grinded. And the quench-cooled samples were stored in a desiccator with silica gel at 4 °C for further analysis.

One gram of two crystalline drugs with a fixed molar ratio (1:1) (CIM-NAP, CIM-IND, NAP-IND) was mixed. Drug mixtures were being milled gently with mortar and pestle for 2 minutes to make sure the two drugs mixed completely, and no amorphous form produced. Then, each of the three mixtures was preformed into co-amorphous form through these steps described above, but the temperature was 165 °C due to the decrease of the melting point after mixing. At last, the prepared samples were stored in a desiccator with silica gel at 4 °C before analysis.

2.3 X-Ray powder diffraction measurement

XRPD was used to study the stability of the crystalline and the amorphous samples [22]. XRPD diagrams were collected using an X-ray diffractometer with Cu-K radiation generated at 45 kV and 40 mA. All the scans were performed with a scanning rate of 2°/min from 5° to 40° at 2θ ranges with a step width of 0.03°.

2.4 Polarized light microscope (PLM) test

To further investigate the drug existing state, three crystalline mixtures and their co-amorphous samples were characterized with a polarized light microscope (PM 6000) connected with a video camera.

2.5 Evaluation of glass transition temperature

To investigate and analyze thermal properties such as melting temperature and glass transition temperature (T_g) [23], differential scanning calorimetry (DSC) measurement was performed with 214-polyma machine. Indium and sapphire were used to calibrate temperature and enthalpy. Nitrogen was used as the protective gas. The sample (5mg) was added into a sealed aluminum pan. The sample was heated from 0 °C to 180 °C at 20 °C/min to establish the T_g of the amorphous forms. The theoretical T_g of the co-amorphous drugs was calculated by the Gordon-Taylor equation,

Biomedical Optics EXPRESS

$$T_{g(mix)} = \frac{w_1 * T_{g1} + K * w_2 * T_{g2}}{w_1 + K * w_2} \quad (1)$$

where $T_{g(mix)}$ is the glass transition temperature of the mixture, w_1, T_{g1}, w_2 and T_{g2} are the weight and glass transition temperature of each component of the co-amorphous drug respectively. The constant K can be further expressed as,

$$K = \frac{\rho_1 * T_{g1}}{\rho_2 * T_{g2}} \quad (2)$$

where ρ_1 and ρ_2 are the density of the co-amorphous components.

2.6 Stability study

The (co-) amorphous drugs were stored in desiccator under dry condition (silica gel) at 4 °C for all the study (180 days). In order to detect the stability of neat amorphous drugs and co-amorphous drugs, samples were analyzed with XRPD at several time points (1 day, 6 days, 20 days and 180 days).

2.7 Raman spectroscopy measurement

Raman spectra were recorded by Xplora microspectrometer (Horiba Scientifics, France) via the LabSpec 6 software, which equipped with liquid N_2-cooled CCD detector. A near infrared laser (785 nm and ~20 mW) was used for excitation. Samples were packed in an aluminium sample holder and spectra were collected at a resolution of 2-3 cm^{-1} with × 50 microscope objectives at room temperature. A baseline correction was applied as pretreatment with the LabSpec 6 software.

2.8 THz spectroscopy measurement

The drug powder was gently grinded with a pestle and mortar to reduce the particle size. Then we mixed the powder with polyethylene (PE) powder (mean particle size 7 to 9 μm) with a pestle and mortar. PE powder is conventionally used as a binder and diluent for THz spectroscopy detection. Subsequently, 0.05 g of drug powder was mixed with 0.05 g of PE powder and pressed (4 t/cm^2 for 1 minute) into pellet. The diameter of pressed pellets was 15 mm which matched the size of the THz light spot and the thickness vary from 0.6 mm to 0.8 mm for the different drugs. A 100% w/w PE tablet was also prepared for background measurement. The absorption coefficients of the drugs were determined with a THz transmission spectrometer (TAS7500SU ADVANTEST Co, Japan). All the measurements were carried out at room temperature, with a nitrogen purge to avoid excess absorption of water vapor. The spectra were measured from 0.5 to 5.0 THz with a good frequency resolution (7.6 GHz).

3. Results and discussion

3.1 Solid-state characterization

At first, the XRPD experiments were used to investigate whether neat drugs (CIM, IND and NAP) and their mixtures (NAP-IND, CIM-IND and CIM-NAP) had been changed into amorphous form through the method described in section 2.2. The results were shown in Fig. 2. As we could see, except the neat NAP, other neat drugs and their binary mixtures presented clear amorphous halo pattern, which meant amorphous drugs were performed.

Biomedical Optics EXPRESS

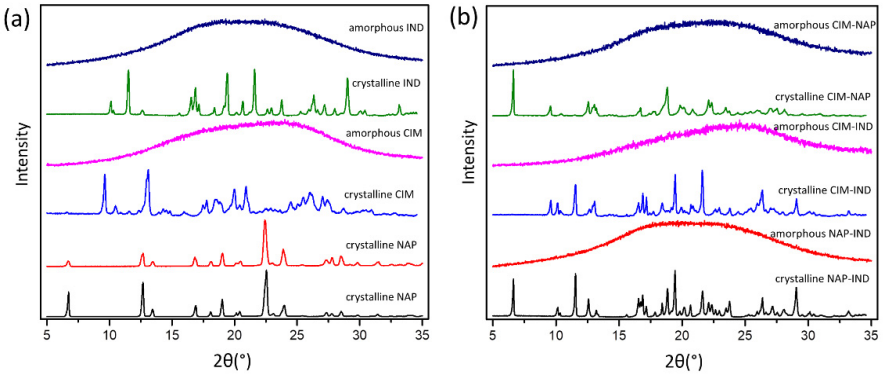

Fig. 2. (a) XRPD patterns of crystalline and amorphous IND, CIM and NAP. (b) XRPD patterns of crystalline and amorphous CIM-NAP, CIM-IND and NAP-IND. All of the drugs presented clear amorphous halo pattern except the neat NAP.

Moreover, we used PLM to make further investigation on the identification of the binary mixing drugs, the results were shown in Fig. 3 and in agreement with the XRPD experiments. The crystalline material was anisotropic and the drug molecules were highly oriented in the crystal and interacted with the polarized light. The brightness of the material was related with the different molecular arrangement orientation in the crystal. In the co-amorphous drugs, we only observed dark field because there was not ordered direction of the molecules in the amorphous form.

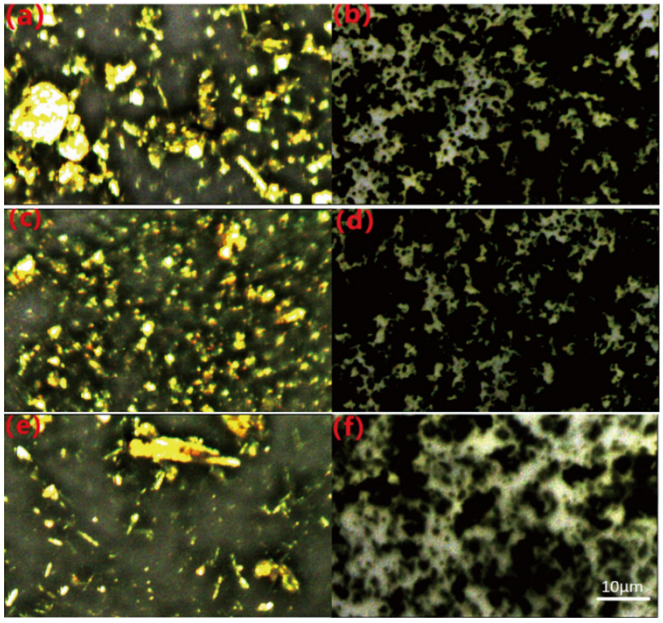

Fig. 3. PLM images of crystalline and quench cooled co-amorphous samples. (a) crystalline CIM-IND, (b) co-amorphous CIM-IND, (c) crystalline NAP-IND, (d) co-amorphous NAP-IND, (e) crystalline CIM-NAP and (f) co-amorphous CIM-NAP.

DSC is a common method to explore the thermodynamic properties of amorphous solid materials, and the appearance of Tg is an indicator of the formation of amorphous form. The results were shown in Fig. 4. Similarly, except for the neat NAP, other samples showed Tgs after quench-cooled method processing, indicating that the amorphous form of these drugs was successfully prepared. Furthermore, the appearance of a single Tg for co-amorphous drug

Biomedical Optics EXPRESS

mixture also indicated the formation of a homogeneous phase that one compound was dissolved in the other one. Indeed, two compounds that were not miscible (or only partially miscible) would show two separate Tgs, one for each compound [24].

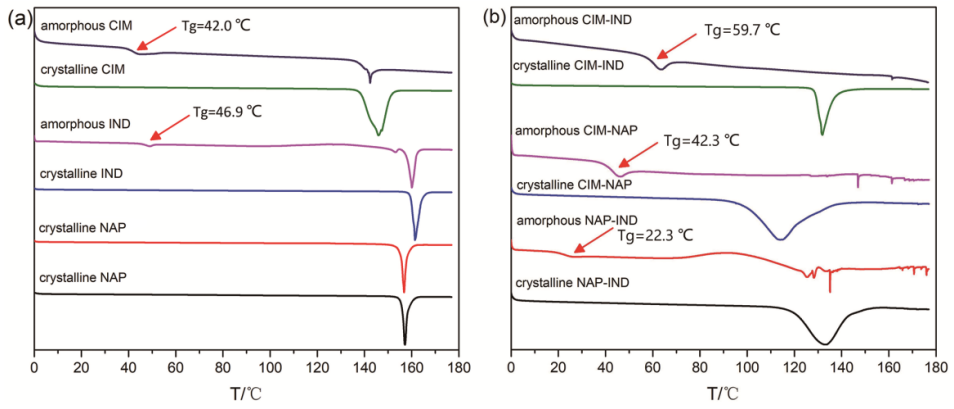

Fig. 4. (a) DSC detection and Tgs of neat crystalline drugs (CIM, NAP, IND). (b) DSC detection and Tgs of co-amorphous mixtures (CIM-NAP, CIM-IND and NAP-IND).

Table 1. Glass transition temperatures of mixtures and single components determined by DSC and calculated values using the Gordon–Taylor equation.

Amorphous Sample	Tg (°C) – Experimental	Tg (°C) – Calculated
CIM	42.0	N/A
NAP	5.0	N/A
IND	46.9	N/A
CIM-NAP	42.3	9.2
CIM-IND	59.7	44.7
NAP-IND	22.3	10.7

In Table 1, we compared the experimental and calculated Tgs of the amorphous samples. The theoretical Tgs of the co-amorphous drugs could be calculated through the Gordon-Taylor equation. The densities of crystalline NAP, amorphous CIM and amorphous IND were 1.263 ± 0.008 g/cm^3, 1.272 ± 0.013 g/cm^3 and 1.380 ± 0.012 g/cm^3 respectively which were determined with a helium pycnometer (AccuPyc 1330 V3.03, US). Since the density of amorphous NAP could not be determined due to its fast recrystallization, the density of crystalline NAP was taken as the value of its amorphous form [25,26]. From the table we can see, the experimental Tgs in trials were much higher than the calculated ones we calculated. Since the Gordon–Taylor equation assumed that there was no interaction between the molecules in the mixture, so the large deviations indicated that there were interactions between the components at the molecular level (discussed below).

3.2 Physical stability evaluation

In order to detect the stability, the (co-)amorphous drugs were characterized through XRPD in 1 day, 6 days, 20 days and 180 days after quench-cooled process. The results of the three neat amorphous drugs were shown in the first row of Fig. 5. Neat CIM has good stability and the amorphous form could last for 180 days with amorphous halo. The amorphous NAP was extremely unstable and converted to crystals in one day completely. And the number of the diffraction peaks of amorphous IND increased with the duration of time and almost transformed into crystalline form after 180 days. As for the co-amorphous drug system (Fig.

Biomedical Optics EXPRESS

5(d), 5(e), 5(f)), it can be seen that the stability is generally stronger than the neat amorphous drugs. Among them, the co-amorphous CIM-NAP was the most stable one, CIM-IND was the second, and the stability of NAP-IND was relatively poor.

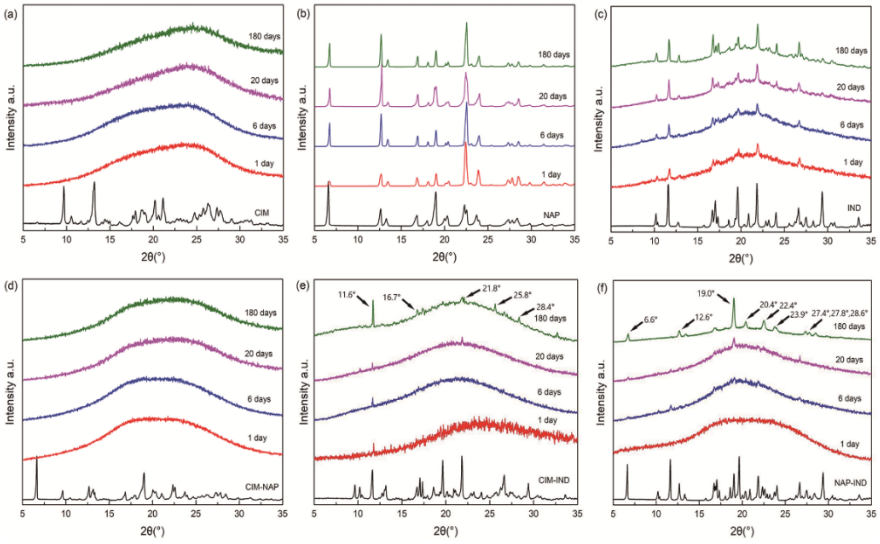

Fig. 5. XRPD patterns of crystalline and co-amorphous samples. (a) quench-cooled CIM, (b) quench-cooled NAP, (c) quench-cooled IND, (d) quench-cooled CIM-NAP, (e) quench-cooled CIM-IND and (f) quench-cooled NAP-IND stored for 1 day, 6 days, 20 days and 180 days at 4°C under dry conditions.

The transformation of drugs from amorphous to crystalline form required a process that could be seen clearly in the XRPD pattern. The results revealed that the converting process of neat amorphous NAP and IND was very fast, while the process of amorphous CIM was much slower. However, when neat drugs were mixed into the co-amorphous form, it was found that the process of transformation was slowed down to a large extent. This phenomenon indicated that the two components of the co-amorphous mixture maybe produce mutual inhibition in the process of converting to the crystalline form. It also could be seen that the instability of the co-amorphous CIM-IND and NAP-IND was mainly caused by the neat amorphous IND and NAP through the corresponding diffraction peaks. This phenomenon was also consistent with the stability of the amorphous CIM, NAP and IND. Furthermore, the co-amorphous CIM-NAP was very stable and the co-amorphous CIM-IND was much more stable than the neat amorphous IND due to the addition of CIM. So, we assumed that the addition of the CIM prevented the amorphous IND or amorphous NAP drug molecules converting into order and kept them in the amorphous form for a longer time. Although the co-amorphous drugs inhibited the transformation from amorphous into crystalline form in some extent, the inhibiting ability was different. Obviously, the inhibiting ability of the co-amorphous CIM-NAP was better than CIM-IND and NAP-IND. The reason was difficult to be directly explained by XRPD as it was related to the molecular interactions.

3.3 Raman spectroscopy measurement

Here, we used the Raman spectroscopy to explore the molecular characteristics and interactions of the amorphous drugs. We focused on changes in some specific Raman peaks to determine the molecular vibrational modes when the drug form changed. The Raman spectra of the three neat drugs in crystalline form and amorphous form were shown in Fig. 6.

Biomedical Optics EXPRESS

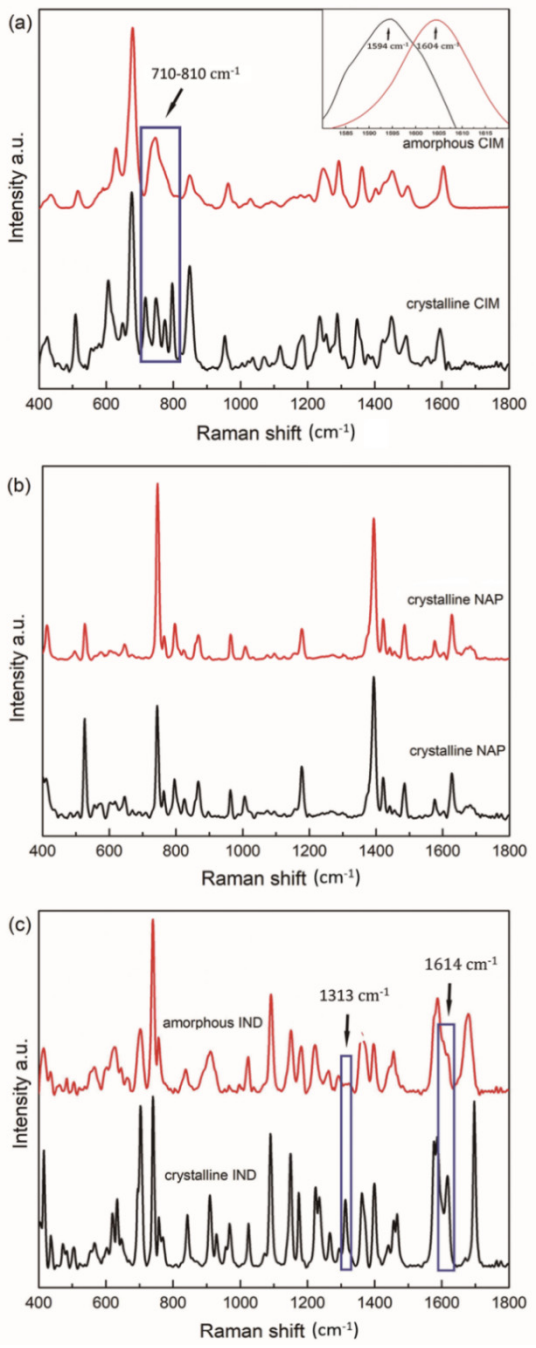

Fig. 6. Raman spectra of neat crystalline and amorphous drugs. (a) amorphous and crystalline CIM, (b) quench-cooled and crystalline NAP, (c) amorphous and crystalline IND.

Biomedical Optics EXPRESS

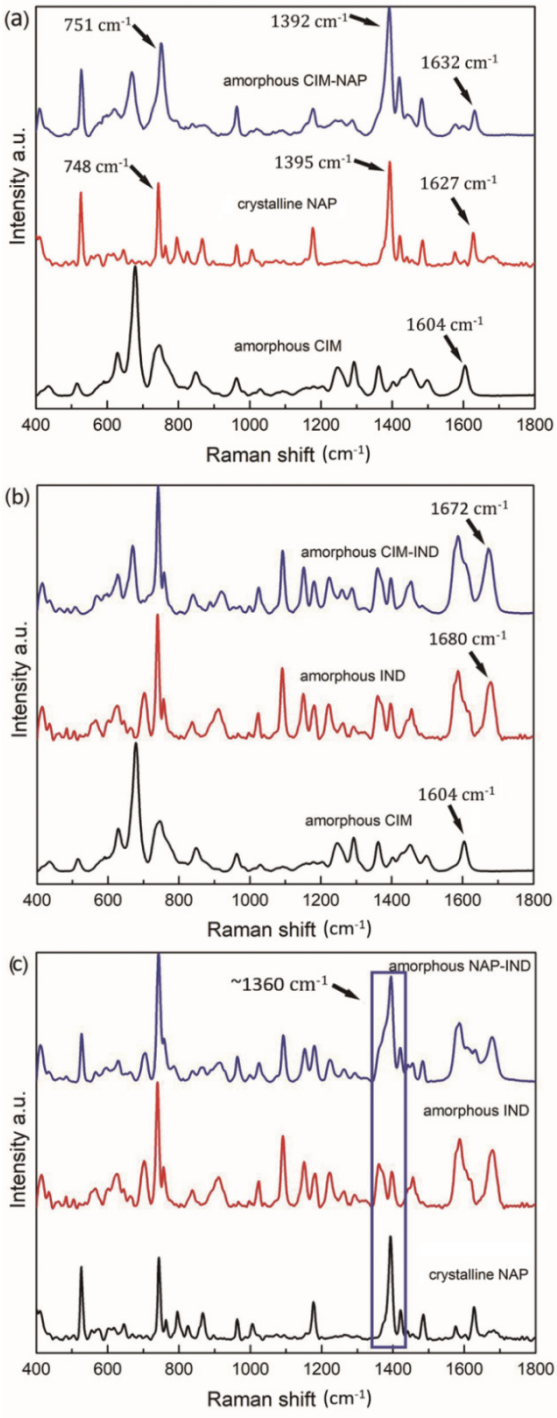

Fig. 7. Raman spectra of co-amorphous drugs and their amorphous components. (a) co-amorphous CIM-NAP, amorphous CIM and quench-cooled NAP; (b) co-amorphous CIM-IND, amorphous CIM and amorphous IND (c) co-amorphous NAP-IND, quench-cooled NAP and amorphous IND.

For neat CIM (Fig. 6(a)), there were two significant differences between the crystalline and amorphous form drugs. Firstly, there were four separated Raman peaks in crystalline

Biomedical Optics EXPRESS

form in the range of 710-810 cm^{-1} (716 cm^{-1}, 749 cm^{-1}, 775 cm^{-1} and 797 cm^{-1}). However, these peaks had been degenerated when it became amorphous form, which were assigned to the secondary aliphatic amines vibration in the molecule [27]. The other variation was the peak shifting from 1594 cm^{-1} of crystal to 1604 cm^{-1} of amorphous form, which was assigned to the vibration of the imidazole ring, indicating that the shift was related to the formation of hydrogen bonds between the imidazole rings. For IND (Fig. 6(c)), the main changes between crystalline and amorphous drugs were the absence of band at 1313 cm^{-1} in the amorphous form and the shift of the band around 1614 cm^{-1}, assigning to the formation of hydrogen bonds between the intermolecular carboxyl groups [27]. Since the amorphous form of NAP was extremely unstable, the transformation in the crystalline form was extremely fast. Thus the Raman features of the amorphous phase did not change much, when compared with the crystalline form (Fig. 6(b)).

Furthermore, we compared the Raman peaks of co-amorphous drugs with their corresponding neat amorphous drugs. We noticed that the Raman spectra of the co-amorphous drugs were not just the accumulation of the neat amorphous components. The results were shown in Fig. 7.

In the co-amorphous CIM-NAP drug, some minor shifts of the CIM bands were observed when compared with the spectra of the neat amorphous CIM (Fig. 7(a)). The ring tensile vibration at 1604 cm^{-1} for the neat amorphous CIM was shifted to 1632 cm^{-1}, suggesting that the imidazole ring of CIM was involved in a solid-state interaction with NAP in the binary amorphous form [27]. On the basis of the above-mentioned band distribution, it appeared that the aromatic ring of NAP was affected by the amorphous process. A shift from 670 cm^{-1} to 666 cm^{-1} associated with C-S-C stretching could also be detected (no clear explanation could be given at the moment). For NAP, several Raman peaks were also shifted. For example, the naphthalene vibration shifted from 1395 cm^{-1} to 1392 cm^{-1}, the vibration of C = C double bond of the naproxen aromatic ring shifted from 1627 cm^{-1} (amorphous) to 1632 cm^{-1} (co-amorphous) and the C-H bending and ring tensile vibrations shifted from 748 cm^{-1} to 751 cm^{-1} [27]. As we observed, new π-π interaction might be formed in the CIM-NAP co-amorphous systems [8,28], which strongly enhanced the stability of the neat amorphous NAP.

Figure 7(b) showed that the differences of the Raman spectra of neat amorphous IND, neat amorphous CIM and co-amorphous CIM-IND.As we could see, the neat amorphous IND compared with the co-amorphous CIM-IND exhibited a shift in the Raman band at 1680 cm^{-1}, which was assigned to the intermolecular carboxyl hydrogen bond indicating that the addition of CIM might influence the formation of hydrogen bonds between the amorphous IND. Meanwhile, the Raman peak at 1604 cm^{-1} was also shifted compared with co-amorphous CIM-IND, which was standard for the vibration of the imidazole ring in CIM [27,29], and its deviation indicated that the vibration had been changed. As the structure of imidazole contained a tertiary carbon atom with lone pair electrons, it bound to protons which had weak basicity. The IND contained a carboxyl group that easily ionizes the proton, and we assumed that during the formation of the co-amorphous, the two drugs had a salt-forming interaction. This effect significantly enhanced the stability of the neat amorphous IND.

It has already demonstrated that the stability of co-amorphous NAP-IND is relatively poor [30]. And it is also reported that these two drugs remain stable by hydrogen bonds between the carboxyl groups in the co-amorphous form through infrared radiation spectra [31]. Our results reached the same conclusion by comparing the changes in their Raman peaks. Compared with neat amorphous IND, co-amorphous NAP-IND had a slight shift at the 1672 cm^{-1} peak, which was assigned to the out-of-plane deformation of the intermolecular carboxyl hydrogen bond. Meanwhile, changes in Raman bands around 1360 cm^{-1} were assigned to the deformation vibration of the hydroxyl in carboxyl [32]. Since the hydrogen bond formation through molecules was extremely weak and easily destroyed, therefore the co-amorphous NAP-IND was relative unstable.

Biomedical Optics EXPRESS

From the results of co-amorphous drugs via Raman spectroscopy, we found that the conversion from amorphous to crystalline form was often accompanied by the formation of new molecular interactions. In the process, the intermolecular energy was reduced and the molecular arrangement became regular. The intermolecular interactions in CIM-NAP included the π-π interactions and hydrogen bonds. The interactions in CIM-IND were mainly the salt formation interactions between the two drug molecules, as well as a series of hydrogen bonds. In the NAP-IND systems, hydrogen bonds were dominant. Since the acting force of the π-π interactions and salt formation were obviously stronger than the hydrogen bonds, it was not surprising that the corresponding co-amorphous system was higher stable. Therefore, we concluded that there were two main factors affecting the stability of the co-amorphous drugs. The main factor is the intensity of interactions between the two components in the co-amorphous form and the other one was the transforming ability of amorphous components into crystalline form.

Biomedical Optics EXPRESS

3.4 THz absorption spectroscopy measurement

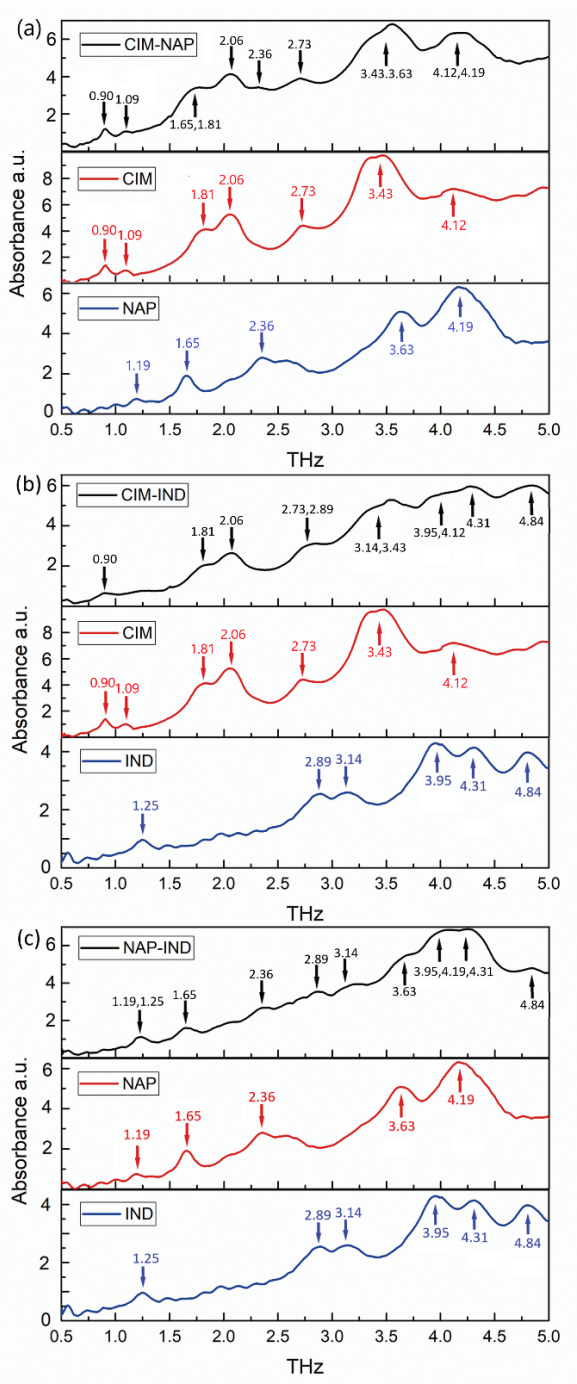

Fig. 8. THz absorption spectra of CIM, NAP, IND and their binary mixed samples at room temperature. (a) crystalline CIM and NAP mixture, (b) crystalline CIM and IND mixture, (c) crystalline NAP and IND mixture. The THz peaks of the crystalline drug mixtures were the accumulation of the THz peaks of each neat crystalline components.

Biomedical Optics EXPRESS

Furthermore, we measured the THz spectra of the three neat crystalline drugs and their binary crystalline mixtures at room temperature (Fig. 8). The results showed that the neat drugs had various THz fingerprint spectra. As the figures show, the THz peaks of crystalline CIM were 0.90 THz, 1.09 THz, 1.81 THz, 2.06 THz, 2.73 THz, 3.43 THz and 4.12 THz. The peaks of crystalline NAP were 1.19 THz, 1.65 THz, 2.36 THz, 3.63 THz and 4.19 THz. The peaks of crystalline IND were 1.25 THz, 2.89 THz, 3.14 THz, 3.95 THz, 4.31 THz and 4.84 THz. And the THz peaks of the crystalline drug mixtures were the accumulation of the THz peaks of each neat crystalline components, although some adjacent peaks overlapped each other indicating that the process of mixing the neat crystalline drugs did not lead to the disappearance of the original interactions [33].

We also measured the THz absorption spectra of the crystalline samples and their corresponding (co-)amorphous ones. The results were shown in Fig. 9. It could be seen that the difference between the crystalline and amorphous phases obviously. After the crystalline drugs became amorphous, the THz absorption coefficients increased generally, and the THz peaks of crystalline samples disappeared gradually. This phenomenon could be explained through the fact that the transformation from the crystalline state to the amorphous form induced a complete vanishing of the original crystalline vibrational modes between molecules. THz spectroscopy was indeed a good method to distinguish the crystalline and amorphous materials.

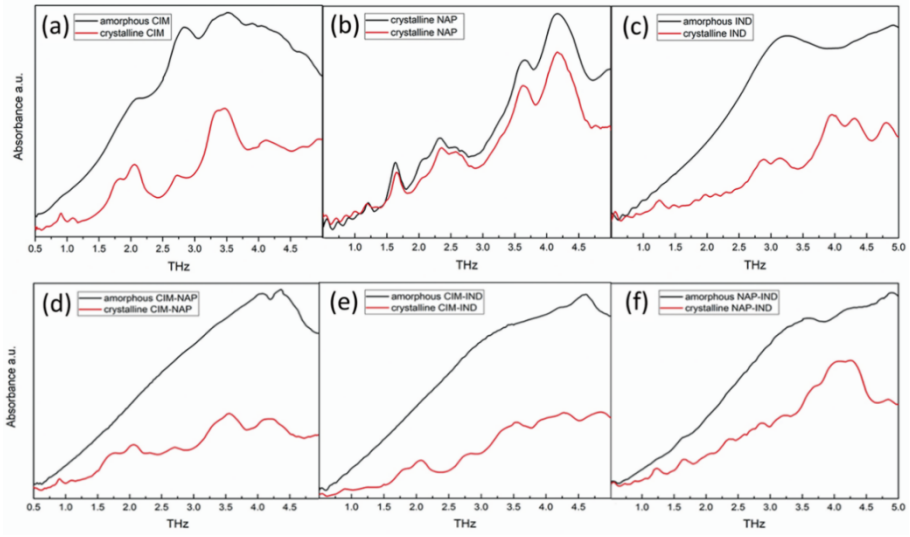

Fig. 9. THz spectra of crystalline and amorphous drugs: (a) amorphous and crystalline CIM, (b) quench-cooled and crystalline NAP, (c) amorphous and crystalline IND, (d) co-amorphous and crystalline CIM-NAP, (e) co-amorphous and crystalline CIM-IND and (f) co-amorphous and crystalline NAP-IND.

4. Conclusions

In this paper, we explored the vibrational properties of co-amorphous drugs in molecular level with Raman and THz spectroscopy. We started from the various stabilities of several amorphous drugs and explored the molecular interactions by vibrational spectroscopy. Raman spectroscopy demonstrated that the force to keep the stability of the three co-amorphous drug systems were mainly π-π interactions, salt formations and hydrogen bonds. Generally, we found that the stability of co-amorphous drugs was better than their neat amorphous components for these samples we tested. Thus we demonstrated that the intermolecular interactions played a crucial role in the transformation of the co-amorphous drugs into the crystalline ones [16]. By performing THz spectroscopy on the co-amorphous sample, we

Biomedical Optics EXPRESS

found that THz spectra could distinguish the crystalline and amorphous drugs more clearly than the Raman spectra. In conclusion, multispectral detection on co-amorphous systems proposed some supplement of the molecular interaction mechanism and provided a direction for the choice of components to improve the stability of amorphous form.

Funding

National Key Basic Research and Development Plan 973 Project (2015CB755400); National High Technology Research Program 863 Program (2015AA021107); Priority projects of the National Natural Science Foundation (81430054); Priority projects of Military Sciences Fund (BWS13C013) (2016XYY08).

Disclosures

The authors declare that there are no conflicts of interest related to this article.

References

1. N. J. Babu and A. Nangia, "Solubility Advantage of Amorphous Drugs and Pharmaceutical Cocrystals," Cryst. Growth Des. **11**(7), 2662–2679 (2011).
2. H. Grohganz, P. A. Priemel, K. Löbmann, L. H. Nielsen, R. Laitinen, A. Mullertz, G. Van den Mooter, and T. Rades, "Refining stability and dissolution rate of amorphous drug formulations," Expert Opin. Drug Deliv. **11**(6), 977–989 (2014).
3. B.C. Hancock and G. Zografi, "Characteristics and significance of the amorphous state in pharmaceutical systems," J. Pharm. Sci. **86**, 1–12 (2010).
4. R. Laitinen, K. Löbmann, C. J. Strachan, H. Grohganz, and T. Rades, "Emerging trends in the stabilization of amorphous drugs," Int. J. Pharm. **453**(1), 65–79 (2013).
5. K. Kawakami, "Modification of Physicochemical Characteristics of Active Pharmaceutical Ingredients and Application of Supersaturatable Dosage forms for Improving Bioavailability of Poorly Absorbed Drugs," Adv. Drug Deliv. Rev. **64**(6), 480–495 (2012).
6. D. E. Alonzo, G. G. Zhang, D. Zhou, Y. Gao, and L. S. Taylor, "Understanding the behavior of amorphous pharmaceutical systems during dissolution," Pharm. Res. **27**(4), 608–618 (2010).
7. K. Löbmann, K.T. Jensen, R. Laitinen, T. Rades, C.J. Strachan, H. Grohganz, "Stabilized Amorphous Solid Dispersions with Small Molecule Excipients," in *Amorphous Solid Dispersions* (Springer, 2014), pp. 613–636.
8. M. Allesø, N. Chieng, S. Rehder, J. Rantanen, T. Rades, and J. Aaltonen, "Enhanced dissolution rate and synchronized release of drugs in binary systems through formulation: Amorphous naproxen-cimetidine mixtures prepared by mechanical activation," J. Control. Release **136**(1), 45–53 (2009).
9. S. J. Dengale, S. S. Hussen, B. S. M. Krishna, P. B. Musmade, G. Gautham Shenoy, and K. Bhat, "Fabrication, solid state characterization and bioavailability assessment of stable binary amorphous phases of Ritonavir with Quercetin," Eur. J. Pharm. Biopharm. **89**, 329–338 (2015).
10. V. Tantishaiyakul, K. Suknuntha, and V. Vao-Soongnern, "Characterization of Cimetidine-Piroxicam Coprecipitate Interaction Using Experimental Studies and Molecular Dynamic Simulations," AAPS PharmSciTech **11**(2), 952–958 (2010).
11. Y. Gao, J. Liao, X. Qi, and J. Zhang, "Coamorphous repaglinide-saccharin with enhanced dissolution," Int. J. Pharm. **450**(1-2), 290–295 (2013).
12. K. Löbmann, R. Laitinen, H. Grohganz, K. C. Gordon, C. Strachan, and T. Rades, "Coamorphous Drug Systems: Enhanced Physical Stability and Dissolution Rate of Indomethacin and Naproxen," Mol. Pharm. **8**(5), 1919–1928 (2011).
13. S. Yamamura, H. Gotoh, Y. Sakamoto, and Y. Momose, "Physicochemical properties of amorphous salt of cimetidine and diflunisal system," Int. J. Pharm. **241**(2), 213–221 (2002).
14. L. M. Martínez, M. Videa, G. A. López-Silva, C. A. de Los Reyes, J. Cruz-Angeles, and N. González, "Stabilization of amorphous paracetamol based systems using traditional and novel strategies," Int. J. Pharm. **477**(1-2), 294–305 (2014).
15. G. P. Johari, S. Kim, and R. M. Shanker, "Dielectric study of equimolar acetaminophen-aspirin, acetaminophen-quinidine, and benzoic acid-progesterone molecular alloys in the glass and ultraviscous states and their relevance to solubility and stability," J. Pharm. Sci. **99**(3), 1358–1374 (2010).
16. S. J. Dengale, H. Grohganz, T. Rades, and K. Löbmann, "Recent advances in co-amorphous drug formulations," Adv. Drug Deliv. Rev. **100**, 116–125 (2016).
17. Y. Du, H. X. Fang, Q. Zhang, H. L. Zhang, and Z. Hong, "Spectroscopic investigation on cocrystal formation between adenine and fumaric acid based on infrared and Raman techniques," Spectrochim. Acta A Mol. Biomol. Spectrosc. **153**, 580–585 (2016).
18. Y. Du and J. Xue, "Investigation of Polymorphism and Cocrystallization of Active Pharmaceutical Ingredients Using Vibrational Spectroscopic Techniques," Curr. Pharm. Des. **22**(32), 4917–4928 (2016).

Biomedical Optics EXPRESS

19. Y. Masubuchi, H. Saito, and T. Horie, "Structural requirements for the hepatotoxicity of nonsteroidal anti-inflammatory drugs in isolated rat hepatocytes," J. Pharmacol. Exp. Ther. **287**(1), 208–213 (1998).
20. S. Emami and C. Gespach, "Pharmacology of histamine H2 receptor antagonists in the human gastric cancer cell line HGT-1. Structure-activity relationship of isocytosine-furan and imidazole derivatives related to cimetidine," Biochem. Pharmacol. **35**(11), 1825–1834 (1986).
21. T. Vasconcelos, S. Marques, J. das Neves, and B. Sarmento, "Amorphous solid dispersions: Rational selection of a manufacturing process," Adv. Drug Deliv. Rev. **100**, 85–101 (2016).
22. S. Thakral, M. W. Terban, N. K. Thakral, and R. Suryanarayanan, "Recent advances in the characterization of amorphous pharmaceuticals by X-ray diffractometry," Adv. Drug Deliv. Rev. **100**, 183–193 (2016).
23. J. A. Baird and L. S. Taylor, "Evaluation of amorphous solid dispersion properties using thermal analysis techniques," Adv. Drug Deliv. Rev. **64**(5), 396–421 (2012).
24. D. J. van Drooge, W. L. J. Hinrichs, M. R. Visser, and H. W. Frijlink, "Characterization of the molecular distribution of drugs in glassy solid dispersions at the nano-meter scale, using differential scanning calorimetry and gravimetric water vapour sorption techniques," Int. J. Pharm. **310**(1-2), 220–229 (2006).
25. B. C. Hancock, G. T. Carlson, D. D. Ladipo, B. A. Langdon, and M. P. Mullarney, "Comparison of the mechanical properties of the crystalline and amorphous forms of a drug substance," Int. J. Pharm. **241**(1), 73–85 (2002).
26. M. Rehman, B. Y. Shekunov, P. York, D. Lechuga-Ballesteros, D. P. Miller, T. Tan, and P. Colthorpe, "Optimisation of powders for pulmonary delivery using supercritical fluid technology," Eur. J. Pharm. Sci. **22**(1), 1–17 (2004).
27. D. A. Long, *Infrared and Raman Characteristic Group Frequencies, Tables and Charts,* 3rd Edition, George Socrates, ed. (John Wiley and Sons, 2010), p. 905.
28. S. J. Dengale, H. Grohganz, T. Rades, and K. Löbmann, "Recent advances in co-amorphous drug formulations," Adv. Drug Deliv. Rev. **100**, 116–125 (2016).
29. S. Yamamura, H. Gotoh, Y. Sakamoto, Y. Momose, "Physicochemical properties of amorphous precipitates of cimetidine-indomethacin binary system," European J. Pharmaceut. Biopharmaceut. **49**, 259–265 (2000).
30. K. Löbmann, R. Laitinen, H. Grohganz, K. C. Gordon, C. Strachan, and T. Rades, "Coamorphous drug systems: enhanced physical stability and dissolution rate of indomethacin and naproxen," Mol. Pharm. **8**(5), 1919–1928 (2011).
31. K. Löbmann, R. Laitinen, H. Grohganz, C. Strachan, T. Rades, and K. C. Gordon, "A theoretical and spectroscopic study of co-amorphous naproxen and indomethacin," Int. J. Pharm. **453**(1), 80–87 (2013).
32. Z. Zhuang, X. Shi, Y. Chen, and M. Zuo, "Surface-enhanced Raman scattering of trans-1,2-bis (4-pyridyl)-ethylene on silver by theory calculations," Spectrochim. Acta A Mol. Biomol. Spectrosc. **79**(5), 1593–1599 (2011).
33. Y. Zhao, Z. Li, J. Liu, C. Hu, H. Zhang, B. Qin, and Y. Wu, "Intermolecular vibrational modes and H-bond interactions in crystalline urea investigated by terahertz spectroscopy and theoretical calculation," Spectrochim. Acta A Mol. Biomol. Spectrosc. **189**, 528–534 (2018).